PHYS 410 Project 2

Kevin Wang

Dec 2, 2024

1 Introduction

In this project, I numerically solved the time-dependent Schrodinger equation under various initial conditions and potential fields. The Schrodinger equation is a PDE that governs the wave-equation of a non-relativistic quantum-mechanical system. Although complex in nature, it shares similarities with the wave equation and heat equation. The numerical models were then used to conduct experiments, demonstrating the accuracy and versatility of the model. In particular, this project highlights the accessibility of numerical simulation, allowing for preliminary visualizations of a theory before physical experimentation.

In the first part of the project, I implement a 1-D model of the Schrodinger equation bounded on the interval $x \in [0,1]$, with discretion via the Crank-Nicholson (CN) method. Such a discretization allows for second-order accuracy in space and time. Computational efficiency is maintained by solving a sparce system of linear equations involving symmetric tridiagonal matrices. Imposed initial conditions include sinusoidal and boosted Gaussian, and imposed potential includes no potential or a rectangular barrier or well. The convergence of the model is verified via a 4-level convergence test involving taking differences between levels and with the exact solution. The model is then applied to finite well and finite barrier problems to draw inferences from the probability function.

In the second part of the project, I generalize the problem to the second dimension, which will allow for a better understanding of the Schrodinger equation. Specifically, I solve the equation in the unit square defined by $(x,y) \in [0,1] \times [0,1]$, with discretization via the alternating-direction implicit (ADI) method. The ADI method is an extension of the CN method, that maintains computational efficiency in a similar manner, cycling through solution passes in each spatial dimension. After the model was implemented, a convergence test similar to the 1-D case was applied. Critically, a second dimension allows for a more visually clear simulation of various physical experiments including barriers, wells, and double-slit interference.

2 Review of Theory and Numerical Approach

2.1 The 1-D Schrodinger Equation

After non-dimensionalization, the continuum equation is

$$i\psi(x,t)_t = -\psi_{xx} + V(x,t)\psi, \tag{1}$$

where the wavefunction, $\psi(x,t)$ is complex. The solution is bounded by the domain

$$0 \le x \le 1, \quad 0 \le t \le t_{max},$$

subject to initial and boundary conditions

$$\begin{aligned} \psi(x,0) &= \psi_0(x), \\ \psi(0,t) &= \psi(1,t) = 0. \end{aligned} \tag{2}$$

(**Eq. 1**) has exact solution

$$\psi(x,t) = e^{-im^2\pi^2 t}\sin(m\pi x) \tag{3}$$

for $V(x,t) \equiv 0$, m is a positive integer. I define a diagnostic quantity, the cumulative integral, $P(x,t)$ of the probability density, $\rho = |\psi|^2 = \psi\psi^*$:

$$P(x,t) = \int_0^x \rho(a,t)da = \int_0^x \psi(a,t)\psi^*(a,t)da. \tag{4}$$

I will not normalize the wavefunction in this project, so $P(1,t)$ will not necessarily be unity. However, it should be conserved to the level of solution error. In this project, the trapezoidal rule will be used to approximate the integral to the level of solution error.

2.2 Crank-Nicholson (CN) Method

The CN discretization combines the forward Euler and backward Euler methods, introducing an intermediate time step in the grid. Sepcifically, for a general PDE of the form

$$\begin{aligned} \psi_t(x,t) &= F(u,x,t,u_x,u_{xx}), \\ \frac{u_i^{n+1} - u_i^n}{\Delta t} &= \frac{1}{2}\left[F_i^{n+1}(u,x,t,u_x,u_{xx}) + F_i^n(u,x,t,u_x,u_{xx})\right] \end{aligned} \tag{5}$$

2.3 CN Discretization of the 1-D Schrodinger Equation

I discretize the continuum domain by introducing the discretization level, l, and the ratio of temporal to spatial mesh spacings $\lambda = \frac{\Delta t}{\Delta x}$. Then I define

$$n_x = 2^l + 1,\ \Delta x = 2^{-l},\ \Delta t = \lambda\Delta x,\ n_t = \lceil\frac{t_{max}}{\Delta t}\rceil + 1.$$

Applying the CN scheme (**5**) to the 1-D Schrodinger equation (**1**), I obtain

$$i\frac{\psi_j^{n+1}-\psi_j^n}{\Delta t}=-\frac{1}{2}\left(\frac{\psi_{j+1}^{n+1}-2\psi_j^{n+1}+\psi_{j-1}^{n+1}}{\Delta x^2}+\frac{\psi_{j+1}^{n}-2\psi_j^{n}+\psi_{j-1}^{n}}{\Delta x^2}+V_j^{n+\frac{1}{2}}\left(\psi_j^{n+1}+\psi_j^n\right)\right), \quad (6)$$

for $j=2,3,...n_x-1,\ n=1,2,...,n_t-1$. The IC and BC's are given by

$$\begin{aligned}\psi_1^{n+1}=\psi_{n_x}^{n+1}=0, \quad n=1,2,\ldots,n_t-1,\\ \psi_j^1=\psi_0(x_j), \quad j=1,2,\ldots,n_x.\end{aligned} \quad (7)$$

Manipulating (**6**) to group terms with time step $n+1$, and noticing that $\forall n, V_j^{n+\frac{1}{2}}=V_j$ since the potential is time-independent, I obtain

$$\begin{aligned}&\left(\frac{i}{\Delta t}-\frac{1}{\Delta x^2}-\frac{1}{2}V_j\right)\psi_j^{n+1}+\frac{1}{2\Delta x^2}\psi_{j+1}^{n+1}+\frac{1}{2\Delta x^2}\psi_{j-1}^{n+1}\\ &=-\frac{1}{2}\left(\frac{\psi_{j+1}^{n}-2\psi_j^{n}+\psi_{j-1}^{n}}{\Delta x^2}\right)+\left(\frac{1}{2}V_j+\frac{i}{\Delta t}\right)\psi_j^n=f_j,\\ &j=2,3,\ldots,n_x-1.\end{aligned} \quad (8)$$

Letting $c_-=c_+=\frac{1}{2\Delta x^2}$ and $c_0=\frac{i}{\Delta t}-\frac{1}{\Delta x^2}-\frac{1}{2}V_j$, and incorporating the IC and BC's, I get

$$\begin{bmatrix}1 & 0 & & & & \\ c_- & c_0 & c_+ & & & \\ & c_- & c_0 & c_+ & & \\ & & \ddots & \ddots & \ddots & \\ & & & c_- & c_0 & c_+\\ & & & & 0 & 1\end{bmatrix}\begin{bmatrix}\psi_1^{n+1}\\ \psi_2^{n+1}\\ \psi_3^{n+1}\\ \vdots\\ \psi_{n_x-1}^{n+1}\\ \psi_{n_x}^{n+1}\end{bmatrix}=\begin{bmatrix}f_1\\ f_2\\ f_3\\ \vdots\\ f_{n_x-1}\\ f_{n_x}\end{bmatrix}. \quad (9)$$

2.4 The 2-D Schrodinger Equation

After non-dimensionalization, the continuum equation is

$$i\psi(x,,yt)_t=-(\psi_{xx}+\psi_{yy})+V(x,t)\psi, \quad (10)$$

where the wavefunction, $\psi(x,t)$ is complex. The solution is bounded by the domain

$$(x,y)\in[0,1]\times[0,1], \quad 0\le t\le t_{max},$$

subject to initial and boundary conditions

$$\begin{aligned}\psi(x,y,0)=\psi_0(x,y),\\ \psi(0,y,t)=\psi(1,y,t)=\psi(x,0,t)=\psi(x,1,t)=0.\end{aligned} \quad (11)$$

(**Eq. 11**) has exact solution

$$\psi(x,t)=e^{-i(m_x^2+m_y^2)\pi^2 t}\sin(m_x\pi x)\sin(m_y\pi y) \quad (12)$$

for $V(x,t)\equiv 0$, m_x,m_y are a positive integers.

2.5 ADI Discretization of the 2-D Schrodinger Equation

Instead of solving a single non-tridiagonal equation, I can solve two sets of tridiagonal equations. I discretize the continuum domain by introducing the discretization level, l, and the ratio of temporal to spatial mesh spacings $\lambda = \frac{\Delta t}{\Delta x} = \frac{\Delta t}{\Delta y}$. Then I define

$$n_x = n_y = 2^l + 1,\ \Delta x = \Delta y = 2^{-l},\ \Delta t = \lambda \Delta x,\ n_t = \lceil \frac{t_{max}}{\Delta t} \rceil + 1.$$

I further define the difference operators

$$\partial_{xx}^h u_{i,j}^n \equiv \frac{u_{i+1,j}^n - 2u_{i,j}^n + u_{i-1,j}^n}{\Delta x^2}$$
$$\partial_{yy}^h u_{i,j}^n \equiv \frac{u_{i,j+1}^n - 2u_{i,j}^n + u_{i,j-1}^n}{\Delta y^2}.$$

Applying the ADI scheme to the 2-D Schrodinger equation (**11**), I obtain

$$\left(1 - i\frac{\Delta t}{2}\partial_{xx}^h u_{i,j}^n\right)\psi_{i,j}^{n+\frac{1}{2}} = \left(1 + \frac{\Delta t}{2}\partial_{xx}^h u_{i,j}^n\right)\left(1 + \frac{\Delta t}{2}\partial_{xx}^h u_{i,j}^n - i\frac{\Delta t}{2}V_{i,j}\right)\psi_{i,j}^n \tag{13}$$

for $i = 2,3,...n_x - 1,\ j = 2,3,...n_y - 1,\ n = 1,2,...,n_t - 1$, and

$$\left(1 - \frac{\Delta t}{2}\partial_{xx}^h u_{i,j}^n - i\frac{\Delta t}{2}V_{i,j}\right)\psi_{i,j}^n = \psi_{i,j}^{n+\frac{1}{2}} \tag{14}$$

for $i = 2,3,...n_x - 1,\ j = 2,3,...n_y - 1,\ n = 1,2,...,n_t - 1$. The IC and BC's are given by

$$\begin{gathered}\psi_{1,j}^n = \psi_{n_x,j}^n = \psi_{i,1}^n = \psi_{i,n_y}^n = 0, \quad n = 1,2,\ldots,n_t - 1, \\ \psi_{i,j}^1 = \psi_0(x_i, y_j), \quad j = 1,2,\ldots,n_x.\end{gathered} \tag{15}$$

To implement (**13-15**) in MATLAB efficiently, I must convert the elementwise operations to matrix operations. Take note that (**13**) can be implemented purely via matrix multiplication and division since the LHS is a matrix multiplication. However, (**14**) cannot because the LHS consists of both matrix multiplication and elementwise multiplication.

Finally, note that I must ensure that the boundary conditions are maintained. To do this, all matrices will have their first and last rows and columns removed. This way, the boundary values will have a weight of zero in the operations. When I zero the boundaries after the matrix operations are complete, I can be confident that doing so will not influence the previous calculations. Thus, the system and the BC will be satisfied. I define for any matrix X,

$$[X] = \begin{bmatrix} 0 & \ldots & 0 \\ \vdots & \hat{X} & \vdots \\ 0 & \ldots & 0 \end{bmatrix}.$$

Define

$$\hat{A} = \frac{i \cdot dt}{h^2} \begin{bmatrix} -1 & 0.5 & 0 & \cdots & 0 & 0 \\ -0.5 & -1 & 0.5 & \cdots & 0 & 0 \\ 0 & -0.5 & -1 & \cdots & 0 & 0 \\ \vdots & \vdots & \vdots & \ddots & \vdots & \vdots \\ 0 & 0 & 0 & \cdots & -1 & 0.5 \\ 0 & 0 & 0 & \cdots & -0.5 & -1 \end{bmatrix}, \tag{16}$$

$$\hat{B} = I + \hat{A}, \tag{17}$$

$$\hat{C} = I - \hat{A}. \tag{18}$$

Then I can write (**13**) as

$$\left[\hat{C}\right]\left[\hat{\psi}^{n+\frac{1}{2}}\right] = \left[\hat{B}\right]\left[\hat{C}\right]\left[\hat{\psi}^{n}\right] + \frac{i\Delta t}{2}\left[\hat{V}^{n}\right] \odot \left[\hat{\psi}^{n}\right], \tag{19}$$

where the RHS can be computed and the intermediate step on the LHS can be solved for via left division. Then, I can write (**14**) as

$$\psi_{i,j}^{n+1} - \frac{i\Delta t}{2}\left(\frac{\psi_{i,j+1}^{n+1} - (2 + \Delta y^2 V_{i,j})\psi_{i,j}^{n+1} + \psi_{i,j-1}^{n+1}}{\Delta y^2}\right) = \psi_{i,j}^{n+\frac{1}{2}}, \tag{20}$$

so for each $j \in \{2, 3, ...n_y - 1\}$,

$$\left(\left[\hat{C}\right] + \frac{i\Delta t}{2}\begin{bmatrix} V_{2,j} & 0 & \cdots & 0 \\ 0 & V_{3,j} & \cdots & 0 \\ \vdots & \vdots & \ddots & \vdots \\ 0 & 0 & \cdots & V_{n_x-1,j} \end{bmatrix}\right)\begin{bmatrix} \psi_{2,j}^{n+1} \\ \psi_{3,j}^{n+1} \\ \psi_{4,j}^{n+1} \\ \vdots \\ \psi_{n_x-2,j}^{n+1} \\ \psi_{n_x-1,j}^{n+1} \end{bmatrix} = \begin{bmatrix} \psi_{2,j}^{n+1/2} \\ \psi_{3,j}^{n+1/2} \\ \psi_{4,j}^{n+1/2} \\ \vdots \\ \psi_{n_x-2,j}^{n+1/2} \\ \psi_{n_x-1,j}^{n+1/2} \end{bmatrix}. \tag{21}$$

3 Results

3.1 1-D Convergence Testing

The differences between solutions of adjacent levels as well as the difference with the exact solution is taken. Then, I take the L-2 norm of each difference across all spatial dimensions (just x in this case), Using $\rho = 4$ for second order accuracy, I scale the results. Indeed, the model converges (**Figure 1**).

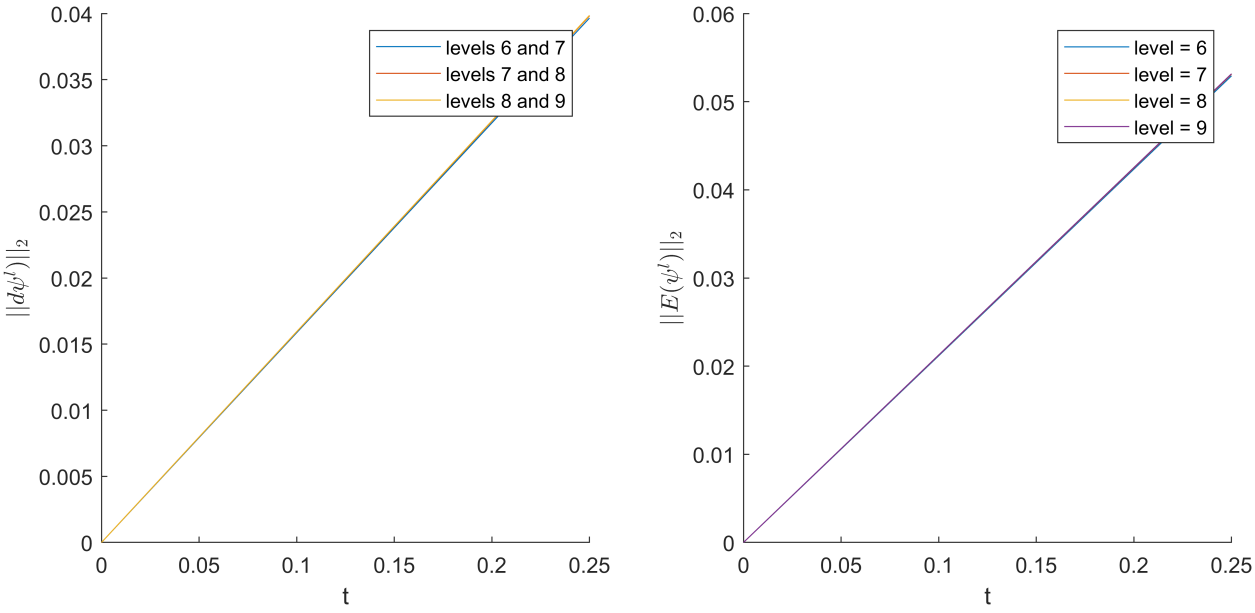

Figure 1: Level Difference Error and Exact Difference Error Over Time For 1-D TISE.

3.2 1-D Experimentation

In this experiment, I varied the potential magnitude of a potential well and a potential barrier, and analyzed their effects on the excess fractional probability. The imposed potential is defined as

$$V(x) = \begin{cases} 0 & \text{if } x < x_{\min} \\ V_C & \text{if } x_{\min} \leq x \leq x_{\max} \\ 0 & \text{if } x > x_{\max} \end{cases},$$

and the excess fractional probability (EFP) is defined as

$$\bar{F}_e(x_1, x_2) = \frac{\bar{P}(x_2) - \bar{P}(x_1)}{x_2 - x_1},$$

where $\bar{P}$ is the temporal average of the running integral of the probability density. In both the barrier and well, the EFP seems to trend downward as the magnitude of the potential increases. Analyzing the barrier first, it's intuitive that the higher the potential barrier, the less chance there is for a particle to tunnel through, thus decreasing the EFP (**Figure 2**). The well is a bit more involved. Although the EFP trends downwards, there are oscillations in the results (**Figure 3**). The downward trend is because the particle has a higher and higher probability of getting trapped in the well when the magnitude of the potential is lower. At certain resonant potentials, the constructive interference of the particle in the well allows some probability of escape. As an analogy, the well is a water bottle. At some shaking frequency, the water may resonant and spill out, depending on the depth of the water bottle.

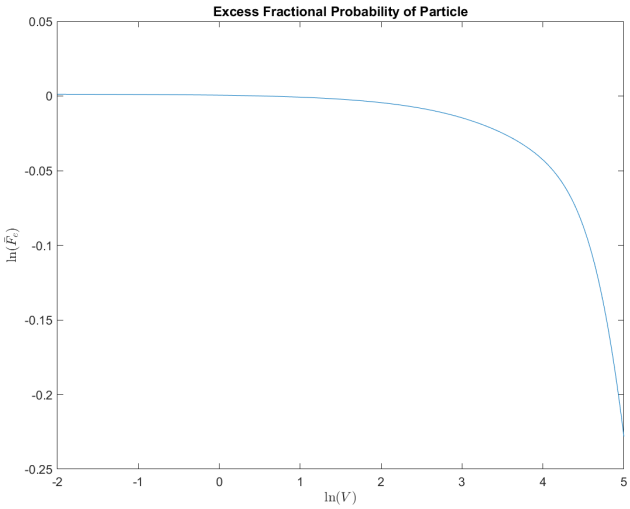

Figure 2: The Relationship Between EFP and Potential With Imposed Potential Barrier

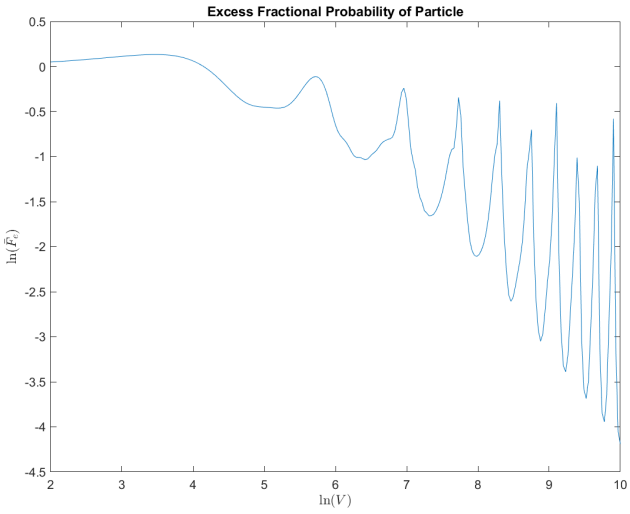

Figure 3: The Relationship Between EFP and Potential With Imposed Potential Well

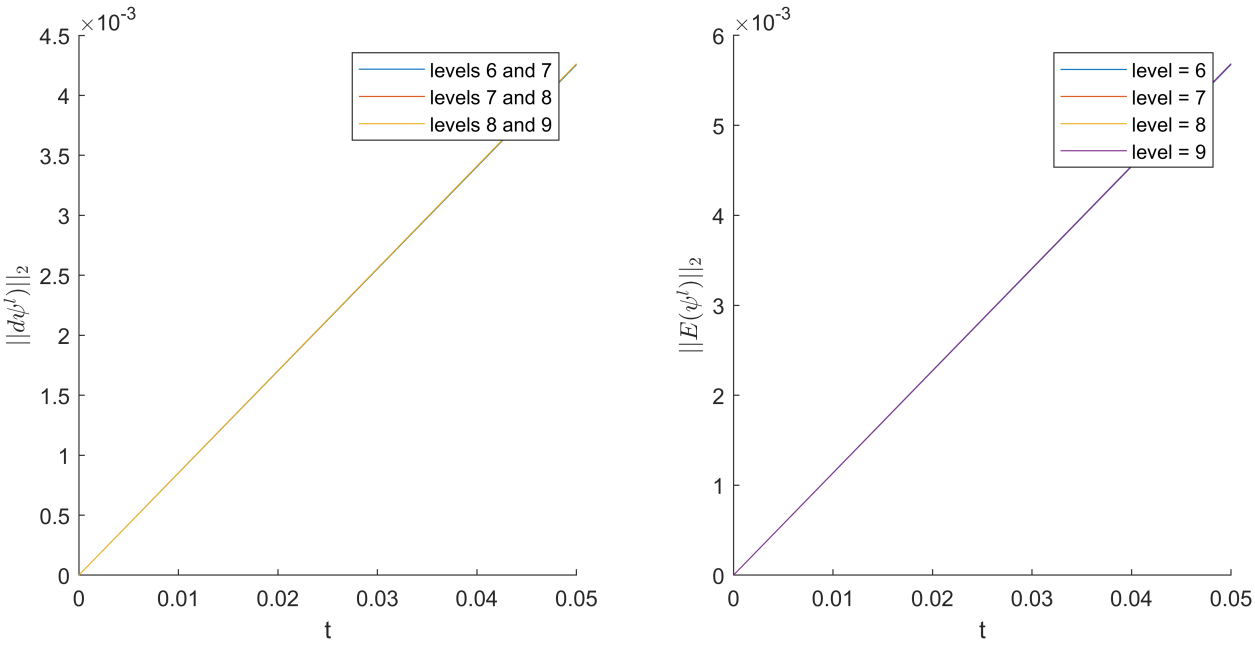

Figure 4: Level Difference Error and Exact Difference Error Over Time For 2-D TISE.

3.3 2-D Convergence Testing

Again, the difference between solutions of adjacent levels as well as the difference with the exact solution is taken. Then, I take the L-2 norm of each difference across all spatial dimensions (just x and y in this case), Using $\rho = 4$ for second order accuracy, I scale the results. Indeed, the model converges (**Figure 4**).

3.4 2-D Experimentation

In this experiment, I examined the propagation of a quantum particle exhibiting wave-like properties. The boosted Gaussian initial condition was used for all trials. I imposed a barrier, well, and double slit.

As expected, the barrier height determines the particle-barrier interaction. If the barrier potential is high, then particles tunnel through a negligible amount (**Figure 5**). However, if the barrier potential is not high enough, the particles have a chance to tunnel through (**Figure 6**). For the well, rather than bouncing off when approaching the well, the wave bounces off when trying to exit the well, leading to the wavefunction being denses inside the well (**Figure 7**). Lastly, the double slit experiment demonstrates that a quantum particle can exhibit self interference (**Figure 8**).

4 Conclusion

In this project, I used the CN method and ADI method to numerically solve the time-independent Schrodinger equation in 1-D and 2-D. I verified that my models converged with second order accuracy in space and time. I then conducted experiments that matched both intuition and quantum

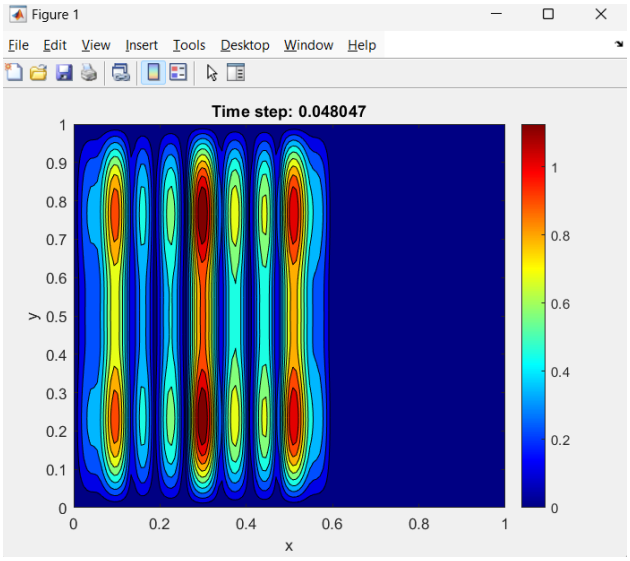

Figure 5: The Magnitude of the Wavefunction Over Space With Well Potential of 1000000000.

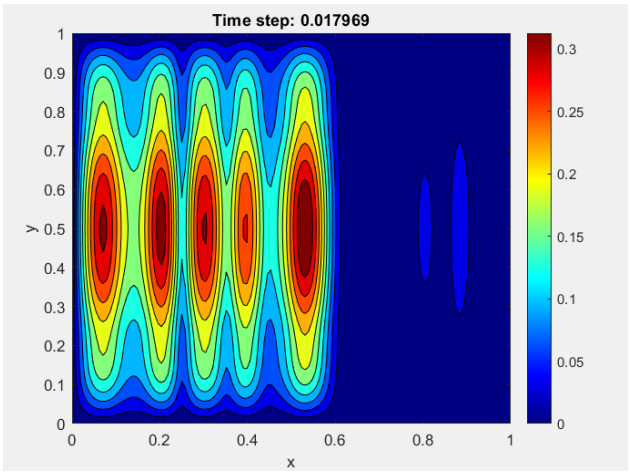

Figure 6: The Magnitude of the Wavefunction Over Space With Well Potential of 5000.

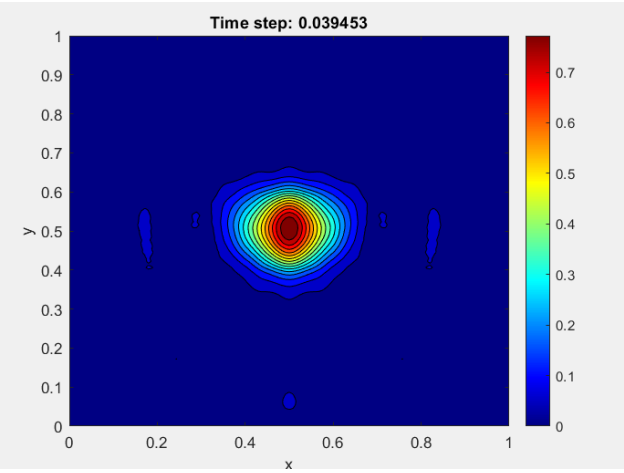

Figure 7: The Magnitude of the Wavefunction Over Space With Well Potential of -1000.

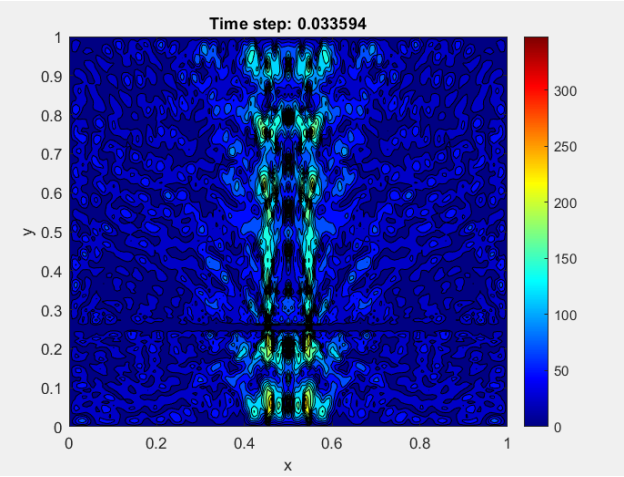

Figure 8: The Magnitude of the Wavefunction Over Space. The $2\Delta y$ thick barrier has a potential of 10000000000 and slits of width 0.005. One slit starts at $x = 0.45$, and the other ends at $x = 0.55$.

theory. This highlights the importance of numerical analysis as an accessible tool both to gain understanding of a theory as well as to draw conclusions.

The 2-D solution was particularly difficult, as the matrix manipulations were complicated and I frequently made errors. Ultimately, I'm am satisfied by the runtime of the program, particularly because I used matrix multiplication rather than row-wise or column-wise operations to solve (**13**).

No generative AI was used in this project.